There is no difference between the EELS spectrum of the adsorbed layer and the IR spectrum of the unadsorbed liquid directly attributable to orientational effects.

Packing densities of TFTP4 were calculated by means of eq 29–32 in Table IV. Packing densities of TFTP2 were calculated from eq 33–35 in Table IV. The results, Tables I and II, resemble those for PFTP. The theoretical packing densities of TFTP4 and TFTP2 are both equal to 0.602 nmol/cm^2 (27.6 Å).

Acknowledgment. This work was supported by the U.S. Department of Energy, Division of Chemical Sciences, Office of Basic Energy Sciences. Instrumentation was provided by the National Science Foundation, Air Force Office of Scientific Research, and the University of Cincinnati.

Spectroscopic Investigations of the Electron Self-Exchange Reaction of the Perchlorate Salt of [1,7-Bis(5-methylimidazol-4-yl)-2,6-dithiaheptane]copper(*n*+) (*n* = 1, 2)

C. M. Groeneveld, J. van Rijn, J. Reedijk, and G. W. Canters*

Contribution from the Gorlaeus Laboratories, Leiden University, P.O. Box 9502, 2300 RA Leiden, The Netherlands. *Received September 23, 1987*

Abstract: The electron self-exchange rate of the perchlorate salt of [1,7-bis(5-methylimidazol-4-yl)-2,6-dithiaheptane]copper(*n*+) (*n* = 1, 2) in dimethyl sulfoxide has been measured by ^{1}H NMR experiments as a function of temperature between 301 and 355 K. The rate amounts to 4 × 10^3 M^{-1} s^{-1} at 301 K. A theoretical analysis of the activation parameters, which amount to $\Delta H^{\ddagger}$ = 9.1 (0.6) kcal/mol and $\Delta S^{\ddagger}$ = −11.8 (1.6) cal/K·mol, shows that the electron-transfer reaction takes place in the adiabatic regime over an electron-transfer distance of 6–7 Å. The dipolar correlation time for the Cu(II) compound amounts to 0.1 ns at 355 K. A Fermi-contact interaction of about 50–100 mG for H2′,2″, H1,5, and Me4′,4″ is compatible with the experimental observations.

Electron self-exchange reactions currently receive considerable attention not only because of their prominent role in the theory of electron transfer but also because they constitute a class of reactions which may provide fundamental insight in the mechanism of electron transfer. Electron self-exchange reactions are inherently simpler to analyze than electron transfer between different redox partners, if only because of the absence of a driving force.

In recent years, a number of studies of electron self-exchange rates of blue-copper proteins have been reported.[1-9] By and large two methods appear applicable to the determination of these rates, first, isotopic labeling (^{63}Cu/^{65}Cu) in combination with rapid flow/freeze techniques[2,4] and, secondly, the NMR study of slightly oxidized solutions of the reduced protein,[1,3,5-9] in cases where the paramagnetic broadening of the NMR signals can be analyzed in the so-called "slow exchange" or "strong-pulse limit".[10,11]

Values of the electron self-exchange rate have been determined experimentally for stellacyanin (1.2 × 10^5 M^{-1} s^{-1} at 293 K),[2] the azurins from *Pseudomonas aeruginosa* (1.3 × 10^6 M^{-1} s^{-1} at 309 K)[3] and *Alcaligenes denitrificans* (4 × 10^5 M^{-1} s^{-1} at 297 K),[6] amicyanin from *Thiobacillus versutus* (8.5 × 10^4 M^{-1} s^{-1} at 309 K),[9] and plastocyanin from French bean ($k \ll 2 \times 10^4$ M^{-1} s^{-1} at 323 K).[1] There is, therefore, appreciable variation in the electron self-exchange rates of blue-copper proteins, and the high values observed for the azurins have especially intrigued researchers.

Electron self-exchange rates of the blue-copper proteins and the corresponding activation parameters are not readily accessible for a thorough theoretical analysis.[12-15] A study of synthetic and relatively simple model compounds may be helpful and important in this respect. Self-exchange reactions have been studied of the following copper compounds: (tri-α-aminoisobutyric acid)copper(*n*+) (*n* = 2, 3) (5.5 × 10^4 M^{-1} s^{-1} at 298 K),[16] [tetrabenzo-[*b,f,j,n*][1,5,9,13]tetraazacyclohexadecine]copper(*n*+) (*n* = 1, 2) (5.5 × 10^5 M^{-1} s^{-1} at 295 K),[17] bis(1,10-phenanthroline)copper(*n*+) (*n* = 1, 2) (∼10^5 M^{-1} s^{-1}),[18] and (2,6-bis([1-((2-pyridin-2-ylethyl)imino)ethyl])pyridine)copper(*n*+) (*n* = 1,2) (1.7 × 10^3 M^{-1} s^{-1} at 298 K).[19] In addition the self-exchange rates of various complexes have been determined indirectly by the application of the Marcus theory[20] on heterogeneous electron-transfer reactions of these complexes with different redox partners.[21-23] By far the fastest reaction, probably proceeding through

---

(1) Beattie, J. K.; Fensom, D. J.; Freeman, H. C.; Woodcock, E.; Hill, H. A. O.; Stokes, A. M. *Biochim. Biophys. Acta* **1975**, *405*, 109–114.

(2) Dahlin, S.; Reinhammar, B.; Wilson, M. T. *Biochem. J.* **1984**, *218*, 609–614.

(3) Groeneveld, C. M.; Canters, G. W. *Eur. J. Biochem.* **1985**, *153*, 559–564; *Rev. Port. Quim.* **1985**, *27*, 145.

(4) Groeneveld, C. M.; Dahlin, S.; Reinhammar, B.; Canters, G. W. *J. Am. Chem. Soc.* **1987**, *109*, 3247–3250.

(5) Groeneveld, C. M.; Canters, G. W. *J. Biol. Chem.* **1988**, *263*, 167–173.

(6) Groeneveld, C. M.; Ouwerling, M. C.; Erkelens, C.; Canters, G. W. *J. Mol. Biol.* **1988**, *200*, 189–199.

(7) Groeneveld, C. M.; Dahlin, S.; Reinhammar, B.; Canters, G. W. *Recl. Trav. Chim. Pays-Bas* **1987**, *106*, 279.

(8) Groeneveld, C. M.; Ouwerling, M. C.; Canters, G. W. *Recl. Trav. Chim. Pays-Bas* **1987**, *106*, 280.

(9) Lommen, A.; Canters, G. W. *Recl. Trav. Chim. Pays-Bas* **1987**, 280.

(10) McLaughlin, A. C.; Leigh, J. S., Jr. *J. Magn. Reson.* **1973**, *9*, 296–304.

(11) Canters, G. W.; Hill, H. A. O.; Kitchen, N. A.; Adman, E. T. *J. Magn. Reson.* **1984**, *57*, 1–23.

(12) Sutin, N. *Acc. Chem. Res.* **1982**, *15*, 275–282.

(13) Sutin, N. *Prog. Inorg. Chem.* **1983**, *30*, 442–498.

(14) Marcus, R. A.; Sutin, N. *Biochim. Biophys. Acta* **1985**, *811*, 265–322.

(15) Newton, M. D.; Sutin, N. *Ann. Rev. Phys. Chem.* **1984**, *35*, 437–480.

(16) Koval, K. A.; Margerum, D. W. *Inorg. Chem.* **1981**, *20*, 2311–2318.

(17) Pulliam, E. J.; McMillin, D. R. *Inorg. Chem.* **1984**, *23*, 1172–1175.

(18) Lee, C. W.; Anson, F. C. *Inorg. Chem.* **1984**, *23*, 837–844.

(19) Goodwin, J. A.; Stanbury, D. M.; Wilson, L. J.; Eigenbrot, C. W.; Scheidt, W. R. *J. Am. Chem. Soc.* **1987**, *109*, 2979–2991.

(20) Marcus, R. A. *J. Phys. Chem.* **1963**, *67*, 853–857.

(21) de Korte, J. M.; Owens, G. D.; Margerum, D. W. *Inorg. Chem.* **1979**, *18*, 1538–1542.

(22) Davies, K. M. *Inorg. Chem.* **1983**, *22*, 615–619.

(23) Karlin, K. D.; Yandell, J. K. *Inorg. Chem.* **1984**, *23*, 1184–1188.

0002-7863/88/1510-4893$01.50/0

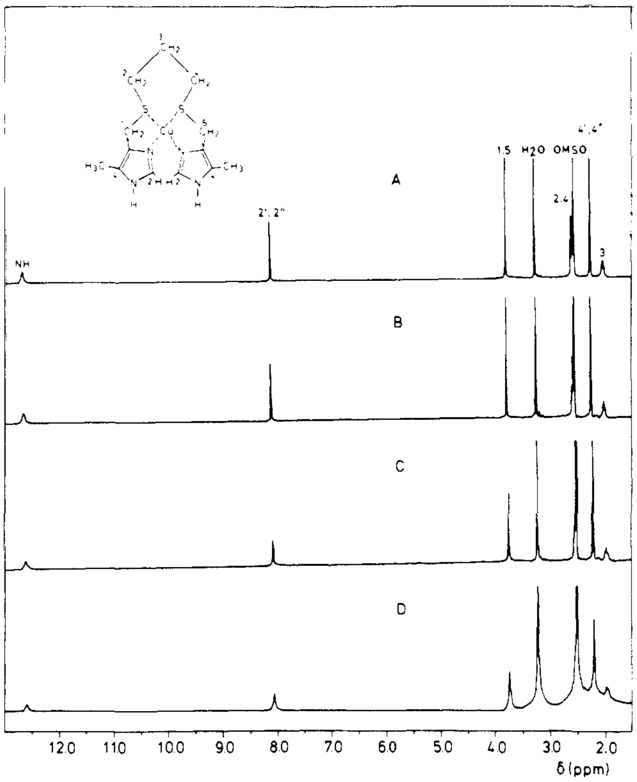

Figure 1. 300 MHz ^{1}H NMR spectrum of Cu(bidhp) in DMSO at various degrees of oxidation, f_p: (A), f_p = 0; (B), f_p = 0.047; (C), f_p = 0.164, and (D), f_p = 0.373. Conditions: 318 K, [Cu(bidhp)$_t$] = 4 mM for $f_p \leq 0.164$ and [Cu(bidhp)$_t$] = 8 mM for f_p = 0.374. In the top spectrum the assignments of all resonances are shown.

an inner-sphere mechanism, is the one observed for copper chloride in 12 N HCl (5×10^7 M^{-1} s^{-1}).[24] All other reports on copper complexes pertain to outer-sphere reactions, which often appear to proceed with rates on the order of 10^3–10^4 M^{-1} s^{-1}. A complicating factor in the analysis is that the copper-coordination geometry may change with the oxidation state[22,23] and that the solvent is often involved in the coordination of the metal.

Recently, the electron self-exchange rate has been reported of a copper complex in which the metal exhibits a five-coordination both in the oxidized and reduced state.[19] Here we report on the results of a ^{1}H NMR study of the electron self-exchange reaction of [1,7-bis(5-methylimidazol-4-yl)-2,6-dithiaheptane]copper(n+) (n = 1, 2) (abbreviated as bidhp:[25] in the rest of the paper Cu$^{\mathrm{I}}$(bidhp) and Cu$^{\mathrm{II}}$(bidhp) will be used as abbreviations for [Cu$^{\mathrm{I}}$(bidhp](ClO$_4$) and [Cu$^{\mathrm{II}}$(bidhp)(H$_2$O)](ClO$_4$)$_2$, respectively[25b]). A schematic drawing of the compound is presented in Figure 1. The crystal structure of the chloride of the Cu(II) form has been reported,[26a] and it appears that the metal is coordinated strongly by two nitrogen atoms. Two sulfur-donor atoms at about 3 Å bind weakly. The chloride ions complete the six-coordinate geometry. In the case of the perchlorate compound, the anions are not bound to the copper, and at best a solvent molecule coordinates to the Cu(II) compound, as found in a few cases.[26b,c] Cu(bidhp) represents the first example of a copper complex with a four-coordination in the reduced as well as the oxidized state of which the electron self-exchange reaction has been studied.

Since specific solvent effects are absent in the system investigated here (vide infra), the compound presents a suitable test case to study the activation parameters of the electron self-exchange reaction within the theoretical framework as reviewed by Sutin and others.[12-15] Moreover, Cu(bidhp) provides for a good model system to test the NMR method for determining electron self-exchange rates. The analysis of the experimental data will be based on the assumption that electron transfer proceeds through an outer-sphere mechanism.[16-23]

Material and Methods

Preparation of Compounds. **[Cu$^{\mathrm{II}}$(bidhp)(H$_2$O)]((ClO$_4$)$_2$).** A solution of 1.1 mmol of copper(II) perchlorate hexahydrate in 10 mL of absolute ethanol was added to a warm solution of the ligand[25a] (1 mmol) in 25 mL of absolute ethanol. The solution immediately turned dark green. Subsequently 4 mL of triethyl orthoformate was added, and the product was precipitated by concentration of the solution to ca. 10 mL and cooling to −20 °C. The precipitate was filtered, collected, and dried in vacuo.

[Cu$^{\mathrm{I}}$(bidhp)](ClO$_4$). The synthesis and all manipulations were carried out under nitrogen in Schlenk-type glassware. The ligand[25a] (1 mmol) was dissolved in 25 mL of absolute ethanol. The solution was refluxed for 1 h under a stream of nitrogen and cooled. Copper(II) perchlorate hexahydrate (0.55 mmol) was dissolved in 20 mL of acetonitrile and reduced with an excess of copper powder (Merck, electrochemically prepared). The mixture was stirred for 1 h and flushed with nitrogen for another hour. The Cu(I) solution was then added to the ligand solution through a glass frit. The mixture was concentrated to 10 mL, whereupon a white precipitate formed. This was filtered by using 20 mL of oxygen-free diethyl ether as the transfer liquid, collected, and dried in vacuo. Both compounds were stored at 4 °C, the former one under N$_2$.

Sample Preparation. NMR samples were made in an N$_2$ atmosphere by mixing the required amount of a solution of Cu$^{\mathrm{I}}$(bidhp) with a solution of Cu$^{\mathrm{II}}$(bidhp) both in 99% DMSO-d_6 (Baker). The NMR samples were carefully sealed off with a rubber cap and parafilm and were maintained under N$_2$ until the time of measurement in order to prevent oxidation by oxygen from the air. It was found that the ordinary DMSO-d_6 solution used for the NMR experiments contained 10 mM H$_2$O. In addition, it should be noted that Cu$^{\mathrm{II}}$(bidhp) contains one water molecule per molecule of Cu$^{\mathrm{II}}$(bidhp), coordinated, in the solid state, to the copper.[25b]

NMR Measurements. NMR spectra were measured on a Bruker WM-300 spectrometer at various temperatures between 28 °C and 82 °C. Free induction decays were accumulated in 8 K and Fourier transformed in 16 K memory after zero filling. Usually 80 scans were stored per spectrum.

T_2^{-1} values were obtained by multiplying line widths at half height by π. T_1 measurements were performed by the inversion recovery method. The peak heights obtained from the spectra were used as input for a three parameter nonlinear least-squares fit to a single exponential to obtain the T_1 value.

Chemical shifts are quoted in parts per million (ppm) downfield from sodium 2,2-dimethyl-2-silapentane 5-sulfonate. The chemical shift of the DMSO-d_5 signal (present as an impurity in the perdeuteriated solvent), which served as an internal reference, was set to 2.50 ppm (the DMSO chemical shift was found to be temperature independent between 28 °C and 82 °C within 0.02 ppm with respect to tetramethylsilane).

Conductivity Measurements. For the conductivity experiments DMSO of ultrapure quality (Baker) was used without further purification. The measurements were performed at 25 °C with a *Radiometer* Conductivity meter, type CDM 2e, and a standard conductivity cell. The temperature during the measurements was maintained at 25 °C with a Haake thermostat. The cell constant, C (cm^{-1}), of the conductivity cell was calibrated by measuring the equivalent conductivity of solutions of KBr (dried by heating under vacuum for several minutes) in DMSO at various concentrations (between 0.3 mM and 3.6 mM) and comparing these data with literature values.[27] The cell constant amounted to 0.84 ± 0.02 cm^{-1}. The conductivity measurements of Cu$^{\mathrm{I}}$(bidhp) were performed in a special experimental setup that allowed for the measurements being performed under an N$_2$ atmosphere.

Results

NMR Spectroscopy. The complete ^{1}H NMR spectrum of Cu$^{\mathrm{I}}$(bidhp) together with the assignments of all the resonances and a schematic drawing of the compound are shown in Figure 1. The proton assignments are based on the chemical shifts, intensities, and multiplet structures of the resonances. At 318 K, the chemical shifts, δ (ppm), amount to the following: NH, 12.60; H2′,2″, 8.07; H1,5, 3.74; H2,4, 2.53; Me4′,4″, 2.19; and H3, 1.95.

The second-order rate constant, k_{ex} (M^{-1} s^{-1}), of the electron self-exchange reaction has been determined by NMR as follows. Under the assumption that the chemical shift of the proton res-

---

(24) McConnell, H. M.; Weaver, H. E. *J. Chem. Phys.* **1956**, *25*, 307–311.

(25) (a) Bouwman, E.; Driessen, W. L. *Synth. Commun.* **1988**, in the press. (b) Rijn, J. van; Ph. D. Thesis, **1985**, Leiden University.

(26) (a) Rijn, J. van; Driessen, W. L.; Reedijk, J.; Lehn, J. *Inorg. Chem.* **1984**, *23*, 3584–3588. (b) Rietmeijer, F. J.; Birker, P. J. M. W. L.; Gorter, S.; Reedijk, J. *J. Chem. Soc., Dalton Trans.* **1982**, *1191*–1198. (c) Addison, A. W.; Rao, T. N.; Reedijk, J.; Rijn, J. v.; Verschoor, G. C. *J. Chem. Soc., Dalton Trans.* **1984**, 1349–1356.

Table I. Values of the Slope s (M^{-1} s^{-1}) for the Selected Protons (NH, H2′, 2″, H1, 5, and Me4′,4″) at Various Temperatures between 301 and 355 K[a] and Values of the Slope s^* (M^{-1} s^{-1})[b]

	$s \times 10^{3}$, M^{-1} s^{-1}				$s^* \times 10^{-3}$, M^{-1} s^{-1}		
T, K	NH	H2′,2″	H1,5	Me4′,4″	H2′,2″	H1,5	Me4′,4″
301	6.7 (1.1)	3.9 (0.4)	4.1 (0.2)	3.4 (0.1)	3.4 (0.6)	5.1 (0.7)	4.3 (0.3)
310	12.3 (1.5)	5.4 (0.7)	5.3 (0.5)	3.8 (0.2)	n.m.[c]	n.m.[c]	n.m.[c]
318	13.7 (2.3)	7.4 (1.0)	7.3 (0.5)	6.1 (0.3)	3.6 (0.7)	3.6 (0.8)	1.5 (0.5)
327	19.5 (1.2)	13.8 (1.3)	11.4 (0.6)	9.7 (0.4)	n.m.[c]	n.m.[c]	n.m.[c]
336	42.0 (3.3)	24.5 (1.9)	18.3 (0.7)	16.1 (0.6)	3.4 (0.8)	2.6 (0.4)	1.7 (0.6)
346	52.0 (1.7)	36.3 (2.0)	33.4 (1.6)	21.7 (0.7)	n.m.[c]	n.m.[c]	n.m.[c]
355	73.5 (6.4)	51.5 (3.1)	39.7 (1.2)	32.0 (1.4)	1.9 (1.3)	1.8 (0.4)	-0.1 (0.3)
r,[d] Å	4.8	3.1	3.8	5.9			

[a] Obtained from the line-broadening experiments performed at $[Cu(bidhp)_t]$ = 4–8 mM. [b] Obtained from experiments in which $[Cu^{II}(bidhp)]$ = 0.8 mM and the total concentration of Cu(bidhp) was varied between 4 and 50 mM (see text). [c] n.m. = not measured. [d] Cu–H distances calculated from the crystal structure of $[Cu^{II}(bidhp)(Cl_2)]$.[26]

onance does not differ in the reduced and oxidized species, the paramagnetic effect on the proton spin relaxation time, ΔT_i^{-1} (s^{-1}) (i = 1, 2), is related to the concentration of the paramagnetic ($[P]$) and diamagnetic species ($[D]$), and k_{ex}, through[10,11,28]

$$\Delta T_i^{-1} = T_{i,\mathrm{obsd}}^{-1} - T_{i,\mathrm{rd}}^{-1} = k_{ex}[P]\,\frac{T_{i,\mathrm{p}}^{-1}}{T_{i,\mathrm{p}}^{-1} + k_{ex}[D]} \qquad (1)$$

in which $T_{i,\mathrm{p}}^{-1} = T_{i,\mathrm{ox}}^{-1} - T_{i,\mathrm{rd}}^{-1}$ (i = 1, 2), and subscripts ox and rd denote the oxidized and reduced species, respectively. Equation 1 has been derived[10,28] for dilute solutions of the paramagnetic particles (fraction, f_p, of paramagnetic species $f_p \lesssim 0.1$). When either the so-called slow- or the so-called fast-exchange limit applies,[10] of which the conditions are given by

$$k_{ex}[T] \ll T_{i,\mathrm{p}}^{-1} \qquad \text{(slow-exchange limit)} \qquad (2a)$$

$$k_{ex}[T] \gg T_{i,\mathrm{p}}^{-1} \qquad \text{(fast-exchange limit)} \qquad (2b)$$

in which $[T]$ denotes the total concentration, the more general (valid for the full range $0 \le f_p \le 1$) and simpler eq 3a and 3b apply

$$T_{i,\mathrm{obsd}}^{-1} = T_{i,\mathrm{rd}}^{-1}\, k_{ex}[P] \qquad \text{(slow-exchange limit)} \qquad (3a)$$

$$T_{i,\mathrm{obsd}}^{-1} = T_{i,\mathrm{rd}}^{-1} + \frac{T_{i,\mathrm{p}}^{-1}}{[T]}[P] \qquad \text{(fast-exchange limit)} \qquad (3b)$$

The latter equations show that a plot of $T_{i,\mathrm{obsd}}^{-1}$ versus $[P]$ results in a straight line with a slope, s (M^{-1} s^{-1}), equal to k_{ex} (slow) or $T_{i,\mathrm{p}}^{-1}/[T]$ (fast). Obviously, determination of whether the slow- or fast-exchange limit obtains is important, since only in the former case can a value of k_{ex} be extracted from the relaxation data.

Determination of the relaxation regime can be performed by inspection of the effect of temperature and $[T]$ on the slope s. In the case of the slow-exchange limit, a variation of $[T]$ does not affect s, while a temperature increase, which is usually accompanied by an increase of k_{ex}, will result in an increase of s. On the other hand, when the fast-exchange limit applies, no change of s is expected upon a variation of temperature, while s will decrease with increasing total concentration $[T]$.

The chance that the *slow-exchange* limit applies for a particular proton increases when the distance of the proton to the paramagnetic center, r, decreases, since both $T_{1,\mathrm{p}}^{-1}$ and $T_{2,\mathrm{p}}^{-1}$ are proportional to r^{-6} according to the Solomon–Bloembergen equations[29,30] (vide infra). On the other hand, the chance that the *fast-exchange* limit applies increases when experiments are performed at high temperature and high $[T]$ (see condition (2b)). This condition is also easier met for T_1 than for T_2 data, since $T_{1,\mathrm{p}}^{-1} \le T_{2,\mathrm{p}}^{-1}$.

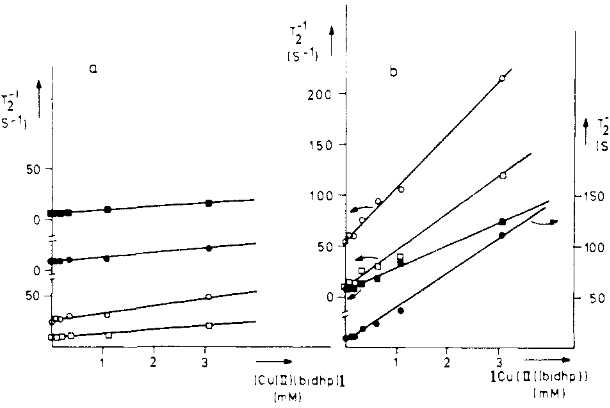

Figure 2. Plot of T_2^{-1} (s^{-1}) versus $[Cu^{II}(bidhp]$ (mM) for the NH proton (○), H2′,2″ (□), H1,5 (●), and Me4′,4″ (■) at 301 K (Figure 2a) and 355 K (Figure 2b). Measurements were performed at $[Cu(bidhp)_t]$ = 4 mM, except the point at $[Cu^{II}(bidhp)]$ = 3 mM for which $[Cu(bidhp)_t]$ = 8 mM.

In the present case, line-broadening experiments were performed on Cu(bidhp) to determine the k_{ex} of the self-exchange reaction. The compound exhibits four free-lying singlets in its NMR spectrum (NH, Me4′,4″, H2′,2″, and H1,5), three of which appeared suitable for line-broadening experiments. The measurements have been performed at total Cu(bidhp) concentrations of 4–8 mM, and the effect of a stepwise increase of the $[Cu^{II}(bidhp)]$ concentration on the line widths of the resonance of the diamagnetic species is shown in Figure 1. The experiments have been performed at various temperatures between 301 and 355 K. As an example, the T_2^{-1} data of the four selected singlets measured at 301 and 355 K are plotted versus the Cu^{II}(bidhp) concentration in Figure 2 (parts a and b, respectively). A least-squares analysis of the data yields the values of s that have been summarized in Table I.

Interestingly, the values of s of the imidazole proton are noticeably larger than for the other protons. The line width of this proton appears not only affected by the electron-transfer reaction but also by a hydrogen exchange with the small amount of water that is present in the DMSO solution.[37b] This is clearly seen in a saturation transfer experiment as illustrated by Figure 3. In this figure the water and imidazole resonances are shown in panel A, and in panel B the same spectrum is shown when the water signal is saturated by irradiation. The saturatin transfer is clearly visible in panel C, which represents the NMR difference spectrum A–B. The signal of the NH proton is, therefore, not used for the determination of k_{ex}.

In the following, the relaxation regime of the T_2 data of the different protons at various temperatures (Table I) is discussed on the basis of the effect of temperature and $[T]$ on s. Additional relaxation time measurements have been performed at high tem-

---

(27) Sears, P. G.; Lester, G. R.; Dawson, L. R. *J. Phys. Chem.* **1956**, *60*, 1433–1436.

(28) Swift, T. J. In *NMR of Paramagnetic Molecules: Principles and Applications*; LaMar, G. N., Dew, W., Horrocks, Jr., Holm, R. H., Eds.; Academic Press: New York/London, 1973; pp 53–83.

(29) Solomon, I.; Bloembergen, N. *J. Chem. Phys.* **1956**, *25*, 261–266.

(30) Dwek, R. A. In *Nuclear Magnetic Resonance in Biochemistry: Applications to Enzyme Systems*; Oxford University Press: New York/London, 1973.

Table II. Spin–Spin Relaxation Data from NMR Experiments Performed at 355 K and with $[\mathrm{Cu(bidhp)_t}] = 50$ mM[a]

proton	r, Å	$T_{2,\mathrm{obsd}}^{-1}$,[b] s^{-1}		$k_{\mathrm{ex}} \times 10^{-4}$, M^{-1} s^{-1}	$T_{2,\mathrm{p}}^{-1} \times 10^{-3}$, s^{-1}	$k[T]$[c] $\times 10^{-3}$		rr[e]	
		$f_\mathrm{p} = 0$	$f_\mathrm{p} = 0.1$[d]			a[f]	b[g]	a[f]	b[g]
H2′,2″	3.1 (0.1)	12.2 (0.3)	203 (10)	5.3	6.3 (0.7)	0.3	2.2	s	s/i
H1,5	3.8 (0.4)	11.1 (0.3)	147 (10)	4.1	3.6 (0.5)	0.3	2.2	s	i
Me4′,4″	5.9 (0.2)	9.2 (0.3)	101 (10)	3.4	1.8 (0.3)	0.3	2.2	s	i

[a] Analyzed by Application of eq 1 (see text). [b] The values between brackets denote estimated errors. [c] $k = 4.3 \times 10^4$ M^{-1} s^{-1}, obtained from the k_{ex} values of H2′, 2″, H1,5, and Me4′,4″. [d] Estimated error: ±10%. [e] rr = relaxation regime. [f] a: $[T] = 8$ mM. [g] b: $[T] = 50$ mM.

Table III. Relaxation Data of NMR Experiments Performed at 355 K and $[\mathrm{Cu(bidhp)_t}] = 50$ mM[a]

proton	T^{-1}, s^{-1}		$T_{1,\mathrm{p}}^{-1} \times 10^{-3}$, s^{-1}	$k[T]$, s^{-1}	rr[b]	$T_{2,\mathrm{dd}}^{-1} \times 10^{-3}$,[d] s^{-1}	$T_{2,\mathrm{Fc}}^{-1} \times 10^{-3}$,[e] s^{-1}	a, mG	
	$f_\mathrm{p} = 0$	$f_\mathrm{p} = 0.1$[c]						$\tau_\mathrm{e} = 1$ ns	$\tau_\mathrm{e} = 3$ ns
$\mathrm{H_{2',2''}}$	2.0 (0.3)	125 (11)	2.5 (0.5)	2.2×10^3	i	3.0 (0.6)	3.2 (0.7)	205	119
$\mathrm{H_{1,5}}$	2.3 (0.2)	87 (4)	1.3 (0.2)	2.2×10^3	i	1.5 (0.2)	2.1 (0.4)	165	95
$\mathrm{Me_{4',4''}}$	1.2 (0.1)	19 (2)	0.18 (0.03)	2.2×10^3	f	0.2 (0.04)	1.7 (0.4)	147	85

[a] Analyzed by application of eq 1, 14, and 15 (see text). [b] rr = relaxation regime. [c] Estimated error: ±10%. [d] Calculated as $1.2 \times T_{1,\mathrm{p}}^{-1}$. [e] Calculated as $T_{2,\mathrm{p}}^{-1} - 1.2 \times T_{1,\mathrm{p}}^{-1}$.

perature and high Cu(bidhp) concentrations, the results of which are subsequently discussed.

When the slow-exchange limit applies, $s = k_{\mathrm{ex}}$, so the values of s for different protons should be equal. Identical values of s are obtained, at low temperatures, for the two protons H2′,2″ and H1,5 situated nearby the copper, while at all temperatures the value of s is slightly smaller for the proton with the largest Cu–H distance (Me4′,4″). It is only above 318 K that the values of s for the former two protons begin to show small differences. These observations indicate that for the H2′,2″ protons the slow-exchange limit applies at least up to 318 K.

The effect of $[T]$ on s has been studied by means of an NMR experiment in which the concentration of the paramagnetic species was kept constant ($[\mathrm{Cu^{II}(bidhp)}] = 0.8$ mM) and the total concentration of Cu(bidhp) was varied between 4 and 50 mM. The results were analyzed by plotting $[\mathrm{Cu(bidhp)_t}](T_{2,\mathrm{obsd}}^{-1} - T_{2,\mathrm{rd}}^{-1})/[\mathrm{Cu^{II}(bidhp)}]$ as a function of $[\mathrm{Cu(bidhp)_t}]$. The slopes, s^* (M^{-1} s^{-1}), of the plots (see Table I) are illustrative since their values should be equal to k_{ex} when the slow-exchange limit applies or to zero when the fast-exchange limit applies. At 301 K, it is observed that $s^* \approx k_{\mathrm{ex}}$ for the different protons, while its value decreases with increasing temperature. Only in the case of the proton with the largest Cu–H distance (Me4′,4″) is the slope, $s^* \approx 0$ at the highest temperature (355 K), which indicates that the fast-exchange limit might be valid for this proton at high temperature and high $[T]$.

In order to obtain more definite clues about the validity of the relaxation regime at high and low Cu(bidhp) concentration, additional line-broadening experiments have been performed at 355 K and $[\mathrm{Cu(bidhp)_t}] = 50$ mM, the results of which are presented in Table II.

The T_2 data at 355 K and $[\mathrm{Cu(bidhp)_t}] = 50$ mM (Table II) and 4–8 mM (Table I) have been analyzed by application of eq 1, which provides for $T_{2,\mathrm{p}}^{-1}$ and k_{ex} at 355 K. The results are presented in Table II, and it is observed that the values of k_{ex} equal s (Table I) for the three protons at 355 K. This demonstrates that the slow-exchange limit does not only apply to the low-temperature $[\mathrm{Cu(bidhp)_t}] = 4$–8 mM T_2 data but also to the high-temperature situation and for all three protons investigated. Consequently at all temperatures used in the low concentration experiments ($[\mathrm{Cu(bidhp)_t}] = 4$–8 mM), $k_{\mathrm{ex}} = s$ for the three protons (Table I).

An average value of k_{ex} of 4.3×10^4 M^{-1} s^{-1} at 355 K is calculated from the data presented in Table II, from which the value of $k_{\mathrm{ex}}[T]$ is calculated and compared with $T_{2,\mathrm{p}}^{-1}$. This allows for a check on the relaxation regime for the T_2 data of the different protons at low and high $[T]$ (see eq 2a and 2b). The results, presented in Table II, confirm that for all three protons at 355 K the slow-exchange limit does apply to the $[\mathrm{Cu(bidhp)_t}] = 4$–8 mM T_2 data, while the intermediate-exchange limit applies for the $[\mathrm{Cu(bidhp)_t}] = 50$ mM T_2 data.

It is observed that the calculated values of k_{ex} for the different protons (Table I) do exhibit small differences, and, apparently, an additional effect contributes to the proton spin relaxation time, the origin of which is presently unknown. However, the variation of k_{ex} is so small that it does not noticeably affect the numerical analysis.

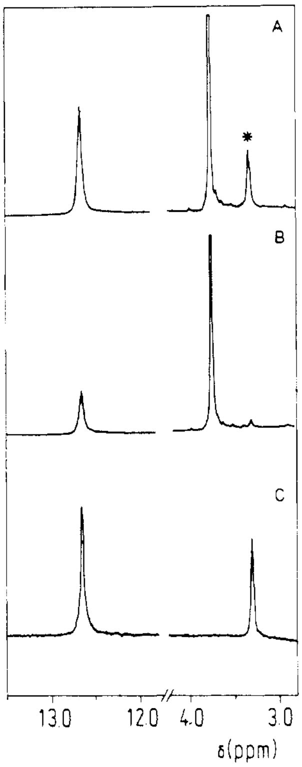

Figure 3. Region of the ^{1}H NMR spectrum of Cu(bidhp) showing the NH ($\delta = 12.60$ ppm) and water resonance ($\delta = 3.29$ ppm) measured in DMSO at 298 K (panel A; the resonance at $\delta = 3.74$ ppm corresponds to H1,5). In panel B the same spectrum is shown when the water resonance is continuously irradiated; in panel C the NMR difference spectrum A–B is shown.

From the k_{ex} values in Table I the activation parameters of the electron-transfer reaction are determined with the Eyring formula

$$k_{\mathrm{ex}} = \frac{kT}{h} e^{-\Delta G^{*}/RT} = \frac{kT}{h} e^{-\Delta H^{*}/RT + \Delta S^{*}/R} \tag{4}$$

in which k is the Boltzmann constant, h the Planck constant, R the gas constant, ΔG^* the free enthalpy of activation, ΔH^* the activation enthalpy, and ΔS^* the activation entropy. The k_{ex} data of all three protons have been used to construct an Eyring plot, and a least-squares analysis of the data points yields $\Delta H^* = 9.1$ (0.6) kcal/mol and $\Delta S^* = -11.8$ (1.6) cal/K·mol.

Finally, NMR experiments were performed in which the spin-lattice relaxation times (T_1) of all three protons were measured at 355 K and at $[\mathrm{Cu(bidhp)_t}]$ = 50 mM, the results of which are presented in Table III. The data are analyzed with eq 1 and $k_{ex} = 4.3 \times 10^4$ M^{-1} s^{-1} (at 355 K), which provided for values of $T_{1,p}^{-1}$ and the relaxation regimes for the various protons. The results are presented in Table III.

Conductivity Measurements. The molar conductivities, Λ_M (Ω^{-1} mol^{-1} cm^2) of Cu^I(bidhp) and Cu^{II}(bidhp), have been measured in DMSO at 25 °C at 1 mM concentration and amount to 35.8 ± 0.3 (Ω^{-1} mol^{-1} cm^2) and 59.2 ± 0.1 (Ω^{-1} mol^{-1} cm^2), respectively. The former value falls in the range of Λ_M = 23–40 Ω^{-1} mol^{-1} cm^2 (1 mM) reported for 1:1 electrolytes in DMSO,[27] and the measured value of Cu^{II}(bidhp) amounts to about twice the value of Cu^I(bidhp). Therefore, both Cu^I(bidhp) and Cu^{II}(bidhp) are thought to be completely dissociated from their anions ($\mathrm{ClO_4^-}$) in DMSO.

Discussion

Water or DMSO Coordination. The results of the conductivity measurements show that the copper complex is probably completely dissociated from its anions, although coordination by water or DMSO might still be possible. To investigate a possible specific coordination of water to Cu^I(bidhp), NMR experiments were performed in which the chemical shift of the water resonance was measured in DMSO solutions containing only Cu^I(bidhp) at various concentrations. It was observed that the chemical shift of the water resonance changes less than 0.01 ppm when [Cu^I(bidhp)] was varied between 4 and 50 mM. Values for the chemical shift difference (of the water resonance) between water bound to an inorganic salt and water free in solution usually amount to 0.5–0.8 ppm.[31,32] The present results implicate that the fraction of bound water molecules amounts to less than 2%, which corresponds to less than 0.2 mM of bound water molecules. Taking into account that at most two water molecules can coordinate to Cu^I(bidhp), the fraction of [Cu^I(bidhp)] to which water is coordinated (at $[\mathrm{Cu(bidhp)_t}]$ = 4–8 mM) amounts to less than 2.5–5%. Unfortunately, a similar analysis to determine whether DMSO coordinates to Cu^I(bidhp) cannot be performed, since the DMSO signal served as an internal reference. However, given the fact that all Cu(I) compounds obtained with bidhp-type ligands, so far, do not contain any coordinating ligands excep bidhp itself, it is highly unlikely that DMSO does coordinate to Cu^I(bidhp).[25] The observation that DMSO does not specifically coordinate to (oxidized) Cu^{II}(bidhp) (vide infra) supports this conclusion.

Whether water specifically coordinates to Cu^{II}(bidhp) or not was investigated by comparing the experimentally obtained line width of the water resonance in Cu^{II}(bidhp) solutions with the theoretical value for water that is coordinated to the Cu^{II}(bidhp). The experimental line width is obtained from the line-broadening experiments on partly oxidized solutions performed at $[\mathrm{Cu(bidhp)_t}]$ = 4–8 mM (data not shown). On the basis of these experiments it is estimated that for a solution containing 3 mM Cu^{II}(bidhp) the broadening of the water resonance amounts to 26 rad/s (at 301 K). Moreover, the resonance sharpens when the temperature is raised, indicating that the signal is an average of the free and possibly bound water. When water would be coordinated to Cu^{II}(bidhp) (assuming a Cu–O distance of 2.2–2.3 Å and a Cu–H distance of 3 Å), its line width would amount to about 1.2×10^4 rad/s (calculated with the Solomon–Bloembergen equations[29,30] and τ_c = 0.1 ns, vide infra). From these figures it can be calculated that about 0.2% of the water molecules present in the solution would be coordinated to Cu^{II}(bidhp). The fraction of Cu^{II}(bidhp) molecules coordinated by water can, therefore, be neglected.

Finally, in order to investigate whether DMSO specifically coordinates to Cu^{II}(bidhp), an additional NMR experiment has been performed in which DMSO-d_6 was titrated with a 100 mM Cu^{II}(bidhp) solution. It was found that the DMSO resonance line width increases linearly with the Cu^{II}(bidhp) concentration (up to 65 mM at 301 K; data not shown). The broadening amounts to 0.19 rad/s·mM Cu^{II}(bidhp) and again decreases with increasing temperature. Calculation of the broadening on the basis solely of translational diffusion[33] leads to nice agreement with experiment (radius DMSO, 2 Å; radius Cu^{II}(bidhp), 5 Å; distance of closest approach, 5 Å, calculated broadening; 0.22 rad/s·mM Cu^{II}(bidhp)).

We conclude that both reduced and oxidized Cu(bidhp) are not specifically coordinated by either water or DMSO, while the copper complex, in both oxidation states, is probably completely dissociated from its anions. Therefore, in the subsequent analysis of the activation parameters the reduced and oxidized metal complex are described as unsolvated particles with charges of +1 and +2, respectively.

Activation Parameters. In this section a numerical analysis of the thermodynamic parameters is presented on the basis of the customary expressions for k_{ex}[12-15]

$$k_{ex} = Kk_{et} \tag{5}$$

$$K = \frac{4\pi N r^2 \delta r}{1000} e^{-w(r)/RT} \tag{6}$$

$$k_{et} = \nu e^{-\Delta G^*/RT} \tag{7}$$

$$w(r) = \frac{3\cdot32\cdot10^{-6}}{D_s}\frac{q_1 q_2}{r} \tag{8}$$

In these expressions K (M^{-1}) is the equilibrium constant for the formation of reactant pairs, N Avogadro's constant, r (cm) the electron-transfer distance, $w(r)$ (kcal/mol) the Coulombic work term for bringing the reactants to the electron-transfer distance r, D_s the static dielectric constant of the medium (46.6 for DMSO), q_i (i = 1, 2) the partial charge on the reaction partner i expressed in electron charges e_o, and k_{et} (s^{-1}) the first-order rate constant for electron transfer inside the reactant pair, while, as we are dealing here with a case of zero driving force, ΔG^* denotes the free enthalpy of activation for electron transfer in the association complex. Furthermore, ν denotes a frequency factor. In the adiabatic regime ν equals a typical nuclear frequency ν_n ($\sim 10^{13}$ s^{-1}) and δr = 2 Å, while in the nonadiabatic regime, ν equals an electronic frequency ν_{el} (s^{-1}) and $\delta r \approx 0.3$ Å.[13] In addition, ΔG^* is related to the reorganization energy, λ, which is subdivided in an inner-shell (λ_{in}) and outer-shell (λ_{out}) part. The outer-shell contribution to ΔG^* is gven by

$$\Delta G^*_{out} = \frac{\lambda_{out}}{4} = \frac{(\Delta e)^2}{4}\left(\frac{1}{a} - \frac{1}{r}\right)\left(\frac{1}{D_{op}} - \frac{1}{D_s}\right) \tag{9}$$

in which Δe is the charge transferred in the reaction, a the radius of the reactants (treated as spheres of equal size), and D_{op} the optical dielectric constant of the medium (equal to the square of the refractive index, n_{DMSO} (= 1.477)).

The inner-shell contribution is given by

$$\Delta G^*_{in} = \frac{\lambda_{in}}{4} = \frac{1}{8}\sum_i f_i \left(\frac{\Delta d_i^o}{2}\right)^2 \tag{10}$$

with f_i the reduced force constant for the ith inner-sphere vibration, and Δd_i^o the corresponding difference in the equilibrium bond distance in the two oxidation states. Combination of eq 4–10 yields the following expressions, by which the experimentally determined parameters ($\Delta G^{\ddagger}$, $\Delta H^{\ddagger}$, $\Delta S^{\ddagger}$) can be related to theoretical parameters (right-hand side of eq 11)

$$\Delta G^{\ddagger} = w(r) + \Delta G^* - RT \ln\left(\frac{A\nu h}{kT}\right) \tag{11}$$

with $A = 4\pi N r^2 \delta r/1000$. Differentation with respect to tem-

---

(31) Shoolery, J. W.; Alder, B. J. *J. Chem. Phys.* **1955**, *23*, 805–811.

(32) Malinowski, E. R.; Knapp, P. S.; Feuer, B. *J. Chem. Phys.* **1966**, *45*, 4274–4279.

(33) Abragam, A. In *The Principles of Nuclear Magnetism*; Oxford University Press: London, 1961.

Table IV. Values for the Contribution of the Work Term ($w(r)$), ΔG^*, and the Preexponential Factor[a] (pre) to the Total Value (tot) of the Activation Parameters of the Electron Self-Exchange Reaction of Cu(bidhp)[b]

				$\Delta H^{\ddagger}$, kcal/mol				$\Delta G^{\ddagger}$, kcal/mol			
	r, Å	$\nu_{el} \times 10^{-9}$, s^{-1}	κ_{el}	$w(r)$	ΔG^{*c}	pre	tot	$w(r)$	ΔG^{*c}	pre	tot
I	5			0.5	8.3	−0.6	8.2	2.9	9.3	0.3	12.5
	6			0.4	7.2	−0.6	7.0	2.4	8.1	0.1	10.6
	7			0.3	6.5	−0.6	6.2	2.0	7.2	−0.1	9.1
	8			0.3	5.9	−0.6	5.6	1.8	6.6	−0.3	8.1
	9			0.3	5.5	−0.6	5.2	1.6	6.1	−0.4	7.3
II	5	5.7×10^4	0.97	0.5	8.3	−0.6	8.2	2.9	9.3	0.4	12.6
	6	2.2×10^3	0.20	0.4	7.2	−0.6	7.0	2.4	8.1	2.1	12.6
	7	1.8×10^2	0.02	0.3	6.5	−0.6	6.2	2.0	7.2	3.4	12.6
	8	3.6×10^1	4×10^{-3}	0.3	5.9	−0.6	5.6	1.8	6.6	4.2	12.6
	9	7.7	8×10^{-4}	0.3	5.5	−0.6	5.2	1.6	6.1	4.9	12.6
exp.							9.1 (0.6)				12.6 (1.1)

[a] pre: see eq 14 and 12. [b] Calculations have been performed for the adiabatic regime (case I) and the nonadiabatic regime (case II) at 298 K. [c] $\Delta G^* = \Delta G^*_{in} + \Delta G^*_{out}$; ΔG^*_{in} = 2 kcal/mol.

perature of eq 11 yields expressions for $\Delta S^{\ddagger}$ and $\Delta H^{\ddagger}$, which are given by

$$\Delta S^{\ddagger} = -\frac{\partial w(r)}{\partial T} - \frac{\partial \Delta G^*}{\partial T} + R \ln\left(\frac{A\nu h}{kT}\right) - R \quad (12a)$$

and

$$\Delta H^{\ddagger} = w(r) - T\frac{\partial w(r)}{\partial T} + \Delta G^* - T\frac{\partial \Delta G^*}{\partial T} - RT \quad (12b)$$

The numerical analysis has been performed as follows. ΔG^*_{in} was estimated by using force constants of 110 and 160 Nm^{-1} [34a] for the two Cu–N and the two Cu–S bonds, respectively. With Δd_i^0 = 0.15 Å an (admittedly crude) estimate of 1–2 kcal/mol is obtained for ΔG^*_{in}.[34b] Both Cu^I(bidhp) and Cu^{II}(bidhp) are treated as spherical particles, with the electron transfer taking place in an association complex in which a is equal to $^1/_2 r$ (see eq 9). For the calculation of $\Delta S^{\ddagger}$, values for the variation of the dielectric constant and refractive index with temperature of DMSO are needed. According to the literature, $\partial n_{\mathrm{DMSO}}/\partial T = -4.4 \times 10^{-4}$ K^{-1} [36] and $\partial D_{s,\mathrm{DMSO}}/\partial T = -0.13$ K^{-1}.[37a]

For the *adiabatic* case, the righ-hand side of eq 11 and 12 can now directly be evaluated for different values of r, and the calculated values of $\Delta G^{\ddagger}$, $\Delta H^{\ddagger}$, and $\Delta S^{\ddagger}$ can directly be compared with experiment (Table IV; row I). For the *nonadiabatic* case, the problem is still underdetermined since apart from r expression 11 contains ν_{el} (see eq 7) as a variable. The calculations for this case were, therefore, performed by setting $\Delta G^{\ddagger}$ in eq 11 equal to the experimental value (12.6 kcal/mol). Introduction of this constraint allows for the calculation of $\Delta S^{\ddagger}$, $\Delta H^{\ddagger}$, and ν_{el} for various values of r (see Table IV). In addition, the electronic transmission factor κ_{el}, given by

$$\kappa_{el} = \frac{2(1 - e^{-\nu_{el}/2\nu_n})}{2 - e^{-\nu_{el}/\nu_n}} \quad (13)$$

was calculated (Table IV). In the nonadiabatic case κ_{el} should be $\ll 1$.

Numerical Analysis of the Relaxation Data. A problem of long standing is whether the sulfur of the coordinating methionine in the blue-copper proteins binds to the copper or not. By measuring the spin distribution on the methionine ligand it would in principle be possible to say something about the strength of this bond. The presence of a Fermi contact interaction can be established by combined T_1 and T_2 measurements. Since these are tedious and difficult to perform on partly oxidized solutions of type I copper proteins, it is worthwhile to study the analogous problem for a model compound. The $T_{i,p}^{-1}$ (i = 1, 2) data presented in Table II will therefore be analyzed in this section. For this analysis use is made of the Solomon–Bloembergen equations,[29,30] the appropriate versions of which are given by

$$T_{1,p}^{-1} = T_{1,dd}^{-1} + T_{1,Fc}^{-1} = \frac{3}{10}\frac{\gamma_I^2 g^2 \beta^2}{r^6}\frac{\tau_c}{1 + \omega_I^2 \tau_c^2} + \frac{1}{2}\frac{\mathrm{A}^2}{\hbar^2}\frac{\tau_e}{1 + \omega_S^2 \tau_e^2} \quad (14a)$$

$$T_{2,p}^{-1} = T_{2,dd}^{-1} + T_{2,Fc}^{-1} = \frac{1}{20}\frac{\gamma_I^2 g^2 \beta^2}{r^6}\left(4\tau_c + \frac{3\tau_c}{1 + \omega_I^2 \tau_c^2}\right) + \frac{1}{4}\frac{A^2}{\hbar^2}\left(\frac{\tau_e}{1 + \omega_S^2 \tau_e^2} + \tau_e\right) \quad (14b)$$

in which $T_{i,dd}^{-1}$ and $T_{i,Fc}^{-1}$ denote contributions from the electron nuclear dipolar interaction and the Fermi-contact interaction, respectively, r represents the electron–nucleus distance, τ_e denotes the electron spin relaxation time, and τ_c is given by $\tau_c^{-1} = (\tau_e^{-1} + \tau_r^{-1})$, τ_r denoting the rotational correlation time of the complex. The other symbols have their usual meaning.

Inspection of eq 14a reveals that with τ_e of the order of 1–3 ns,[38] $T_{1,p}^{-1}$ is governed entirely by $T_{1,dd}^{-1}$; consequently, equating $T_{1,p}^{-1} = T_{1,dd}^{-1}$ provides for an estimate of τ_c. It should be kept in mind that the Solomon–Bloembergen equations are based on the point dipole approximation; a better approximation is obtained when the full electron nucleus dipolar tensor is used in the relaxation equations.[39] For large Cu–H separations, however, the difference between the two approximations becomes small. Equation 14 a is, therefore, applied to the data obtained for the proton with the largest Cu–H distance (Me4′,4″), resulting in a value of the correlation time of $\tau_c = (1.0 \pm 0.2) \times 10^{-10}$ s at 355 K.

The correlation time can also be calculated from $\tau_c^{-1} = \tau_e^{-1} + \tau_r^{-1}$, in which τ = 1–3 ns[38] and τ_r is given by the Stokes–Einstein equation,[33] $\tau_r = V\eta/kT$, in which V denotes the molecular volume and η the viscosity of the solution. Substitution of $V = 3.2 \times 10^5$

---

[34] (a) Thamann, T. J.; Frank, P.; Willis, L. J.; Loehr, T. M. *Proc. Natl. Acad. Sci. U.S.A.* **1982**, *79*, 6396–6400. (b) In this estimate it is implicitly assumed that the normal coordinates of eq 10 to a large extent coincide with localized bond modes. Although customary,[34a,35] this practice is questionable, and the calculated value of ΔG^*_{in} must be used with caution.

[35] Brunschwig, B. S.; Ehrenson, S.; Sutin, N. *J. Phys. Chem.* **1986**, *90*, 3657–3668.

[36] Sears, P. G.; Siegfried, W. D.; Sands, D. E. *J. Chem. Eng. Data* **1964**, *9*, 261–263.

[37] (a) Casteel, F. J.; Sears, P. G. *J. Chem. Eng. Data* **1974**, *19*, 196. (b) On the assumption that the hydrogen exchange proceeds according to a bimolecular reaction mechanism, the apparent bimolecular rate constant, k_H, of the hydrogen exchange between the imidazole and water resonance can be estimated by measuring the line width of the water resonance as a function of [Cu^I(bidhp)] and applying the eq $T_{2,obsd}^{-1} = T_{2,0}^{-1} + k_H[\mathrm{Cu^I(bidhp)}]$. In this eq the term $T_{2,0}^{-1}$ denotes the hypothetical imidazole proton line width in the absence of exchange. From the experimental values of k_H the activation parameters for the hydrogen exchange were found to amount to $\Delta H^{\ddagger}$ = 5.0 (0.8) kcal/mol and $\Delta S^{\ddagger}$ = −28.5 (2.6) cal/K·mol. A further analysis of the data has to await experiments in which the water concentration is varied.

[38] Goldberg, M.; Pavlovic, V.; Pecht, I. *Biochemistry* **1980**, *19*, 5181–5188.

L/mol[26] and $\eta = 0.83$ cp for DMSO at 355 K[36] yields $\tau_R = 9 \times 10^{-11}$ s and, eventually, $\tau_c = (0.9 \pm 0.1) \times 10^{-10}$ s which is in good agreement with the value determined above.

From eq 14a and 14b one finds (with $\omega_I = 1.9 \times 10^9$ rad/s) that

$$\frac{T_{2,\mathrm{dd}}^{-1}}{T_{1,\mathrm{dd}}^{-1}} = \frac{7}{6} + 2.36\tau_c^2 \tag{15}$$

in which τ_c is expressed in ns. With $\tau_c = 0.1$ ns, it follows that $T_{2,\mathrm{dd}}^{-1}/T_{1,\mathrm{dd}}^{-1}$ equals 1.2. On the other hand, from the data presented in Tables II and III one finds values for $T_{2,\mathrm{ox}}^{-1}/T_{1,\mathrm{ox}}^{-1}$ in the range of 2.5–10.4, implying that the Fermi-contact interaction contributes to the spin–spin relaxation time. Its contribution can be calculated by subtraction of $T_{2,\mathrm{dd}}^{-1} = 1.2T_{1,\mathrm{dd}}^{-1}$ (eq 15 with $\tau_c = 0.1$ ns) from the experimental $T_{2,\mathrm{p}}^{-1}$ value. The values obtained in this way for $T_{2,\mathrm{dd}}^{-1}$ and $T_{2,\mathrm{Fc}}^{-1}$ are presented in Table III. The Fermi-contact contribution is equal to $A^2\tau_e/4\hbar^2$ (see eq 14b), in which A is related to the hyperfine splitting constant a (Gauss) by $A = \gamma_e a$. The calculations have been performed with $\tau_e = 1$ and 3 ns, and the results have also been presented in Table II. It is observed that values around 100 mG ($\tau_e = 3$ ns) for the different protons are obtained, with a slightly larger value for H2′,2″.

Conclusion

The first aim of the present study was to see how well the NMR method would perform for determining electron self-exchange rates in the case of a system that would be relatively simple to analyze. The crucial point in the analysis appears to find out whether the observed paramagnetic broadening can correctly be described by the slow-exchange limit. A reliable indication for this limit is when all signals from protons close to the paramagnetic center broaden equally fast. The temperature effect on the broadening, on the other hand, which is often used to check the applicability of the slow-exchange limit is less reliable. When the NMR signals sharpen with temperature in most cases the fast-exchange limit will obtain, but when they broaden either the slow- or the intermediate-exchange regime may hold. The effect of dilution can also be helpful in deciding on the relaxation regime. When the slope s^* of a dilution plot equals the slope s of a line width plot, this is a fairly reliable indication that the slow-exchange limit applies.

In the intermediate-exchange regime, T_2 data can still be analyzed by applying eq 1. This means introduction of a second unknown parameter, $T_{2,\mathrm{p}}^{-1}$, and, consequently, requires additional data by which an independent variable, for instance, the total concentration, is varied. This was done in the present study for the data analyzed in Table II. It is pointed out that a more complete expression for the line-broadening contains a term $\Delta\omega^2$ in the numerator and denominator of eq 1.[11] Here $\Delta\omega$ denotes the shift difference between the resonances in the oxidized and reduced species, and it may contain contributions due to charge effects (Cu^+ or Cu^{2+}), pseudocontact and Fermi-contact interactions. For Cu compounds only the latter term may become non-negligible. A proton hyperfine splitting constant (hfsc) of 100 mG, for instance, produces a Fermi-contact shift on the order of 10^4 rad/s at 300 MHz. In the present case, inclusion of the $\Delta\omega^2$ term in the relaxation formula would not affect the analysis of the data in the slow-exchange limit, but it would lead to somewhat smaller values of $T_{2,\mathrm{p}}^{-1}$ (see Table II) and concomitantly smaller values of the hfsc. According to a rough estimate, inclusion of the $\Delta\omega$ term would diminish the hfsc of the H2′,2″ protons by about 50% from the value reported in Table II and would affect the hfsc of the H1,5 and Me4′,4″ protons even more. A better estimate of proton hfsc than the values presented in Table III would, therefore, amount to 50–100 mG for the H2′,2″ proton, while for the other protons 50 mG would constitute an upper limit.

The analysis of the relaxation data in Table III shows that it is possible indeed to extract information about the presence of spin density of the Cu ligands from combined T_1 and T_2 measurements, provided that fast-exchange limit pertains. This means (see eq 3) that the experiments should be performed at high temperature ($T \geq 50$ °C), high total protein concentrations (>10 mM) and, if possible, in the presence of electron exchange rate enhancing compounds like ferri/ferro cyanide (Lommen, A.; Canters, G. W., unpublished results). High temperatures will also help in reducing τ_c, which in turn will enhance the Fermi contact contribution to the line width relative to the dipolar contribution (see eq 14 and 15).

The second aim of the present study was to investigate the mechanism of the electron self-exchange reaction. It is clear from the data in Table IV (row II) that the *nonadiabatic* case leads to unsatisfactory results. For large separations of the reactants ($r \geq 7$ Å) the partitioning of ΔG^* over ΔH^* and ΔS^* strongly deviates from experiment. For smaller values of r the electronic transmission factor begins to approach 1, which is at variance with the assumption of nonadiabaticity. On the other hand, in the *adiabatic* limit (Table IV, row I), with r in the range of 6–7 Å, there is a good match between the experimental and theoretical values of ΔG^* and between the predicted and experimentally found partitioning of ΔG^* over ΔS^* and ΔH^*, although this match may be somewhat fortuitous in view of the uncertainties associated with the estimate of $\Delta G^*_{\mathrm{out}}$ and especially ΔG^*_{in}. A value of 6–7 Å for the Cu–Cu distance in the encounter complex seems somewhat low in view of the value of 4.9 Å estimated for the effective diameter of the Cu(bidhp) (calculated[35] as $(a_1a_2a_3)^{1/2}$, $a_1 = 13.6$, $a_2 = 11.2$, and $a_3 = 6.0$ Å being the diameters of the Cu(bidhp) along three mutually perpendicular directions[26]). It should be kept in mind, however, that the Cu(bidhp) complex has a highly aspherical and open structure. Model building shows that association complexes are possible in which the Cu–Cu distance is less than 3 Å. This might explain the relatively short electron-transfer distance found in the theoretical analysis.

What bearing do the present results have on the electron self-exchange reaction of blue-copper proteins. It is illustrative to consider the case of the azurins. In these proteins the copper is completely buried inside the protein; on the other hand, in Cu(bidhp) the metal is easily accessible. Yet the electron self-exchange rate of the azurins is about 2 orders of magnitude larger than that of Cu(bidhp) (10^6 versus 10^4 M^{-1} s^{-1}). What then are the factors that favor the self-exchange in the azurins compared to Cu(bidhp)? A possible answer may be found in the data of Table IV. It appears that there are three important contributions to the free enthalpy of activation. The energy required to bring the reactants together symbolized by $w(r)$ provides for a contribution to ΔG^* mainly consisting of an unfavorable entropy term. For azurin, on the other hand, it has been argued that the redox partners associate along the so-called hydrophobic patch on their protein surface, which provides for a large favorable (positive) entropy term. The two other contributions to ΔG^* are as important and consist of the inner- and outer-sphere reorganization energy. As argued above, a reasonable estimate of the inner-sphere reorganization energy amounts to $\Delta H^*_{\mathrm{in}} = 1$–$2$ kcal/mol for the Cu(bidhp) complex. In the azurin, where the differences in the equilibrium geometry around the copper between the reduced and oxidized protein are on the order of 0.05 Å,[40,41] ΔH^*_{in} will be smaller assuming conformational changes in the rest of the protein to be negligible. Finally, the sizable contribution from the outer-sphere reorganization energy to ΔG^* in the present case is due to the high static dielectric constant of DMSO. Again, with the proteins the situation is different. In the association complex of two azurin molecules, assuming water molecules have been squeezed out from the interface region, the effective static dielectric constant will be much closer to the value inside the core of globular proteins ($D_s = 1$–5)[42] than to the value of the surrounding medium, which again lowers the reorganization barrier and enhances the rate of electron transfer compared to the case of Cu(bidhp). This inference can be tested by studying the electron self-exchange of

---

(39) Canters, G. W.; de Boer, E. *Mol. Phys.* **1974**, *27*, 665–687.

(40) Groeneveld, C. M.; Feiters, M. C.; Hasnain, S. S.; Rijn, J. van; Reedijk, J.; Canters, G. W. *Biochim. Biophys. Acta* **1986**, *873*, 214–227.

(41) Groeneveld, C. J.; Aasa, R.; Reinhammar, B.; Canters, G. W. *J. Inorg. Biochem.* **1987**, *31*, 143–154.

(42) Schulz, G. E.; Schirmer, R. H. In *Principles of Protein Structure*; Cantor, C. R., Ed.; Springer-Verlag: New York, 1978.

J. Am. Chem. Soc. 1988, 110, 4900–4905

Cu(bidhp) in a solvent with a low dielectric constant.

Acknowledgment. Two of us (C.M.C. and G.W.C.) gratefully acknowledge useful discussions with Dr. N. Sutin. F. B. Hulsbergen skillfully assisted in the preparation of the samples. We thank Dr. C. J. Bloys van Treslong for permission to use the conductivity equipment in his group.

Registry No. [Cu^{II}(bidhp)](ClO$_4$)$_2$, 114397-75-0; [Cu^{I}(bidhp)](ClO$_4$), 114422-74-1.

Torsional Angles in Vinylarenes Determined by High-Field NMR Spectroscopy

Kevin L. Facchine, Stuart W. Staley,* Peter C. M. van Zijl, Prasanna K. Mishra, and Aksel A. Bothner-By*

Contribution from the Department of Chemistry, Carnegie Mellon University, Pittsburgh, Pennsylvania 15213. *Received November 27, 1987*

Abstract: High-resolution deuterium NMR spectra of styrene-α-d, styrene-d_8, 1-vinylnaphthalene-α-d, and 2-vinylnaphthalene-α-d in hydrocarbon solvents were recorded at field strengths of 14.11 to 14.57 T. Quadrupolar splittings were observed as a consequence of magnetic field-induced alignment of the solute molecules. The magnitudes of the splittings were used to calculate the average value of $\sin^2 \alpha$, where α is the dihedral angle between the vinyl and ring planes; $\alpha_{rms} = \sin^{-1} \langle \sin^2 \alpha \rangle^{1/2}$ was 16.5 ± 0.9° for styrene, 18.3 ± 3.1° for 2-vinylnaphthalene, and 41.8 ± 4.1° for 1-vinylnaphthalene. The styrene value was used to deduce the magnitude of the twofold rotational barrier (4.0 $\pm ^{+0.4}_{-0.3}$ kcal/mol) and the extent of steric destabilization of the planar form. The results are compared with available literature data.

The characterization of the conformation of and internal rotation in styrene (**1**) and substituted styrenes has been investigated by a large variety of techniques, including microwave,[1] infrared,[2] Raman,[2,3] ultraviolet,[4] fluorescence,[3d,5] photoelectron,[6] and NMR spectroscopy,[7] molecular rotatory polarization,[8] calorimetric[9] and molecular refractometric[10] studies, molecular mechanics calculations,[11] and semiempirical[12] and ab initio molecular orbital calculations.[13] The consensus from these investigations is that the internal rotation in styrene is governed largely by a twofold barrier with the planar form being the most stable. However, the magnitude of the barrier is not very well determined, with values from 1.5 to 4.4 kcal mol^{-1} being deduced or calculated (Table I). It is also not clear whether a steric destabilization of the planar form occurs,[14] resulting in a shifting of the energy minimum from α = 0° (α is the dihedral angle between the planes of the vinyl group and the phenyl ring) to α = ±20 to 30°.

Table I. Experimental and Theoretical Rotational Barriers and C_1C_7 Torsional Frequencies for Styrene

method	phase	rotational barrier[a]	ν_{tor}[b]	ref
experimental				
statistical-thermodynamic	gas	2.2	~69	9, 3b
Raman	gas	1.78 ± 0.02	127.7[c]	3b
NMR	liquid	1.6 ± 0.3		7a
NMR	liquid crystal		80	7b
fluorescence, Raman	gas	3.06 ± 0.02	43	3d
NMR	liquid	$4.0 \pm ^{0.4}_{0.3}$	76	this work
theoretical				
STO-3G		4.4		13a
MM2		1.5		11
(5,2/2) contracted		3.9		13b
PPP/σ potential function			99	12c
CNDO/2		4.3		12d
INDO		3.0–3.1		12e
C-INDO		3.65		12f
6-31G		3.1		13c
4-31G		2.8		13d

[a] In kcal mol^{-1}. [b] Fundamental C_1C_7 torsional frequency in cm^{-1}. [c] Two-quantum transition; see also ref 5b.

---

(1) (a) Ralowski, W. M.; Mjöberg, P. J.; Ljunggren, S. O. *J. Mol. Struct.* **1976**, *30*, 1. (b) Ralowski, W. M.; Mjöberg, P. J.; Ljunggren, S. O. *J. Mol. Struct.* **1976**, *31*, 169. (c) Ralowski, W.; Wettermark, G.; Ljunggren, S. *Acta Chem. Scand.* **1973**, *27*, 1565.

(2) Fateley, W. G.; Carlson, G. L.; Dickson, F. E. *Appl. Spectrosc.* **1968**, *22*, 650.

(3) (a) Singh, B.; Dhawan, J. B.; Jaiswal, R. M. P. *Ind. J. Phys.* **1973**, *47*, 69. (b) Carreira, L. A.; Towns, T. G. *J. Chem. Phys.* **1975**, *63*, 5283. (c) Hollas, J. M.; Musa, H.; Ridley, T.; Turner, P. H.; Weisenberger, K. H.; Fawcett, V. *J. Mol. Spectrosc.* **1982**, *94*, 437.

(4) (a) Suzuki, H. *Bull. Chem. Soc. Jpn.* **1960**, *33*, 619. (b) Hollas, J. M.; Khalilipour, E.; Thakur, S. N. *J. Mol. Spectrosc.* **1978**, *73*, 240.

(5) (a) Grajcar, L.; Baudet, J. *J. Mol. Struct.* **1977**, *38*, 121. (b) Hollas, J. M.; Ridley, T. *Chem. Phys. Lett.* **1980**, *75*, 94.

(6) (a) Maier, J. P.; Turner, D. W. *J. Chem. Soc., Faraday Trans. II* **1973**, *69*, 196. (b) Kobayashi, T.; Yokota, K.; Nagakura, S. *J. Electron Spectrosc. Relat. Phenom.* **1973**, *2*, 449.

(7) (a) Schaefer, T.; Parr, W. J. E. *J. Mol. Spectrosc.* **1976**, *61*, 479. (b) Emsley, J. W.; Longeri, M. *Mol. Phys.* **1981**, *42*, 315. (c) Laatikainen, R.; Kolehmainen, E. *J. Magn. Reson.* **1985**, *65*, 89.

(8) Castan, P.; Lopez, A.; Martino, R. *Tetrahedron* **1979**, *35*, 1093.

(9) Pitzer, K. S.; Guttman, L.; Westrum, F. E., Jr. *J. Am. Chem. Soc.* **1946**, *68*, 2209.

(10) Zaitsev, B. A. *Izv. Akad. Nauk, Ser. Khim.* **1973**, 1968.

(11) Allinger, N. L.; Sprague, J. T. *J. Am. Chem. Soc.* **1973**, 95, 3893.

(12) (a) Favini, G.; Simonetta, M. *Theor. Chim. Acta* **1963**, *1*, 294. (b) Hamer, G. K.; Reynolds, W. F. *J. Chem. Soc., Chem. Commun.* **1971**, 1218. (c) Sühnel, J.; Gustav, K. *Z. Chem.* **1977**, *17*, 342. (d) Janssen, J.; Lüttke, W. *J. Mol. Struct.* **1979**, *55*, 265. (e) Momicchioli, F.; Baraldi, I.; Bruni, M. C. *Chem. Phys.* **1982**, *70*, 161. (f) Baraldi, I.; Momicchioli, F.; Ponterini, G. *J. Mol. Struct.* **1984**, *110*, 187.

(13) (a) Hehre, W. J.; Radom, L.; Pople, J. A. *J. Am. Chem. Soc.* **1972**, *94*, 1496. (b) Almlöf, J. E.; Isacsson, P. U.; Mjöberg, P. J.; Ralowski, W. M. *Chem. Phys. Lett.* **1974**, *26*, 215. (c) Bock, C. W.; Trachtman, M.; George, P. *Chem. Phys.* **1985**, *93*, 431. (d) Schaefer, T.; Penner, G. H. *Chem. Phys. Lett.* **1985**, *114*, 526.

(14) (a) Ralowski, W. M.; Mjöberg, P. J.; Almlöf, J. E. *J. Chem. Soc., Faraday Trans. II* **1975**, 1109. (b) Schaefer, T.; Penner, G. H. *Chem. Phys. Lett.* **1985**, *114*, 526.

0002-7863/88/1510-4900$01.50/0